

# 1060. Lamb wave temperature compensation method based on adaptive filter ADALINE network

Lei Qiu<sup>1</sup>, Shenfang Yuan<sup>2</sup>, Tianxiang Huang<sup>3</sup>

State Key Laboratory of Mechanics and Control of Mechanical Structures

Nanjing University of Aeronautics and Astronautics, 29 Yudao Street, Nanjing 210016, China

<sup>2</sup>Corresponding author

E-mail: <sup>1</sup>ql19830925@nuaa.edu.cn, <sup>2</sup>ysf@nuaa.edu.cn, <sup>3</sup>xiang39@nuaa.edu.cn

(Received 10 June 2013; accepted 4 September 2013)

**Abstract.** One of the key issues that need to be addressed in current PZTs array and Lamb wave based Structural Health Monitoring (SHM) methods are the influence of environmental conditions, especially temperature. A new temperature compensation method based on adaptive filter adaptive liner neural (ADALINE) network including a tapped delay line has been developed to compensate the amplitude-change and phase-shift due to temperature. Network construction and procedure of compensation are discussed. The advantage of this temperature compensation method is that only a few baselines are required for a large temperature range. Experiments are conducted on a stiffened carbon fiber composite panel to verify the temperature compensation method under a large temperature range from  $-40\text{ }^{\circ}\text{C}$  to  $80\text{ }^{\circ}\text{C}$ . Results show that this method can compensate for both  $S_0$  mode and  $A_0$  mode. Damage image results show that after the compensation great accuracy for Lamb wave-based damage detection is achieved.

**Keywords:** structural health monitoring, Lamb wave, temperature compensation, adaptive filter ADALINE network.

## 1. Introduction

Much attention has been paid to piezoelectric transducers (PZTs) array and Lamb wave based SHM method because this method is sensitive to inner small damage of composite structures, can monitoring large-scale structures and can be used to damage and impact monitoring [1, 2]. However, current PZTs array and Lamb wave based SHM method depends on the baseline signal acquired under the health status of the monitored structure. The status of the structure can be determined by comparing the baseline signal and monitoring signal with some SHM algorithms [3, 4]. Such a process can be implemented well in laboratory for the steady environmental and operational conditions (EOC). But in practical applications, the monitoring signal is often affected by the changing EOC, which will lead to false monitoring result even the structure is under health status [5-7].

Temperature has shown to be the most influential EOC to SHM methods [8, 9]. Over the last several years, a variety of methods for compensating the temperature effect of Lamb wave acquired by PZTs have been proposed.

(1) Temperature compensation method based on baseline signal stretch (BSS) and optimal baseline subtraction (OBS) has been studied by many researchers [10-14]. In BSS method, the baseline signal is stretched or compressed by a stretch factor to match the monitoring signal. The stretch factor is determined by short time cross-correlation criterion. Though this method requires only one baseline signal and one reference temperature, it is limited to be used in a small range of temperature changes (the maximum temperature changes relative to the reference temperature is  $\pm 2\text{ }^{\circ}\text{C}$ ) [12]. On the other hand, this method can be only used to compensate the phase of Lamb wave signal, while the amplitude of the signal is also temperature sensitive according to many researches and it is important for damage monitoring. In OBS method, a big amount of baseline signals at each reference temperature (the interval of reference temperatures is  $1\text{ }^{\circ}\text{C}$  typically) in the application temperature range must be obtained under health status first. For example, if there are 20 actuator-sensor channels constructed by PZTs array and the application temperature range is  $-40\text{ }^{\circ}\text{C}$  to  $80\text{ }^{\circ}\text{C}$ , the number of the baseline signals is up to  $121 \times 20$ . The optimal baseline signal

for the monitoring signal is selected according to the criterion of mean square deviation. This method requires many baseline signals to achieve a promising compensation accuracy. But in many applications, it may be impossible to obtain the baseline signals with the required temperature resolution. The combination of BSS and OBS can optimally compensate temperature effects and the temperature resolution is optimized to 5 °C [13]. In other words, the number of the baseline signals can be reduced to 25×20. All the studies mentioned above are performed on metallic structures.

(2) The second method is based on wavelet transform and numerical simulation [14]. In this method, wavelet transform of time-frequency domain is performed to Lamb wave signal to decompose it into many Gabor atoms which are temperature compensated. And then, the temperature compensated Lamb wave signal is obtained by wavelet reconstruction based on these atoms. Though this method needs small amount of baseline signals, the mechanism and process is complicated and it is only validated by compensating the direct wave of Lamb wave signal on an aluminum plate currently.

(3) Temperature compensation method based on physical modeling is also studied by many researchers [15-18]. They try to construct a comprehensive Lamb wave propagation model to predict the full pitch-catch Lamb wave signals under changing temperature. Numerical versus experimental studies demonstrate that the high accuracy of temperature compensation of Lamb wave signals can be obtained on metallic structures. But to the application of composite structures, the accuracy physical model is difficult to be acquired.

To develop a temperature compensation method of simple, small amount of baseline signals requiring, high accuracy, large range of temperature applicable and can be used to composite structures easily, this paper proposes a temperature compensation method of Lamb wave signal based on adaptive filter ADALINE (ADaptive LIner NEural, ADALINE) network.

## 2. Experimental research of temperature influence on composite structure

In this section, temperature influence of Lamb wave propagating on a composite structure is studied by an experiment. The structure and the experimental procedure are given out first. And then, temperature influence of different central frequencies of  $A_0$  mode and  $S_0$  mode of Lamb wave signals are discussed. The signals acquired in the experiment are also used to study and validate the temperature compensation method in section 3 and section 4, respectively.

### 2.1. Composite specimen and experimental step

In this paper, a stiffened carbon fiber composite panel of thickness 2 mm is adopted to study the temperature influence and the compensation method as shown in Fig. 1. PZTs (thickness 0.5 mm, diameter 8 mm, PIC255, PI L. P.) are mounted to the surface of the composite panel by using the epoxy adhesive 353ND (Epoxy Technology, Inc). The thickness of the adhesive layer is 0.08 mm approximately. 20 actuator-sensor channels are defined.

An environmental chamber Challenge 250 (Angelantoni Industrie SpA) which temperature controlling accuracy is  $\pm 0.3$  °C is adopted to simulate the temperature environment of PZTs. An integrated structural health monitoring system (ISS) [19] is adopted to fulfill the multi-channel scanning, frequency sweeping and Lamb wave signals acquiring of the 20 actuator-sensor channels constructed by the PZT sensors. In order to study the temperature influence of Lamb wave signals of different central frequencies, a five cycle sine burst is used as an excitation signal whose central frequency is swept from 50 kHz to 500 kHz with an interval of 50 kHz. The sampling rate is 10 MHz.

The temperature cycling in the experiment is performed in the following processes as illustrated in Fig. 2.

(1) Temperature pre-cycling. Temperature is continuously increased from 20 °C to 80 °C. Then it is continuously decreased to -40 °C. Finally, temperature is continuously increased from

-40 °C to 20 °C. The temperature pre-cycling is repeated for three times.

(2) Temperature cycling under health status. Temperature is continuously decreased from 20 °C to -40 °C with a cooling rate of 5 °C/min and kept for 30 min at -40 °C. And then, temperature is increased from -40 °C to 80 °C with a heating rate of 1 °C/min and kept for 30 min at 80 °C. Then, temperature is decreased from 80 °C to -40 °C with a cooling rate of 1 °C/min and kept for 30 min at -40 °C. The Lamb wave signals are acquired from -40 °C to 80 °C and 80 °C to -40 °C of 2 °C interval. Temperature cycling under health status is repeated for three times.

(3) Temperature cycling under damage status. A 100 g mass is bonded in the center of the area surrounded by PZT 5, PZT 6, PZT 8 and PZT 9 by 353ND to simulate damage. The temperature cycling is the same with temperature cycling under health status.

Through this experiment, Lamb wave signals under health and damage status at different temperatures and different central frequencies are acquired. As temperature cycling under health status is repeated for three times, six groups of Lamb wave health signals are acquired, including three in heating stage and three in cooling stage. In each temperature, there are six Lamb wave signals collected at different cycles. They are used as six samples to train and test the network in section 3.

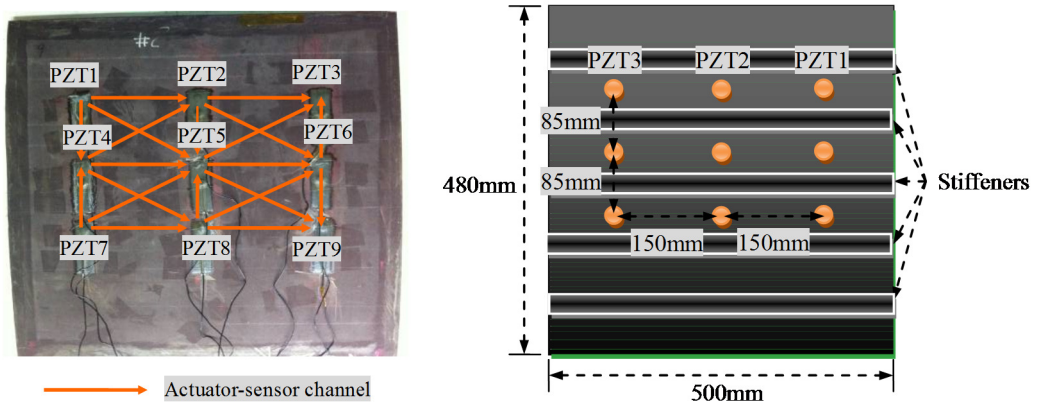


Fig. 1. Composite panel and PZTs placement

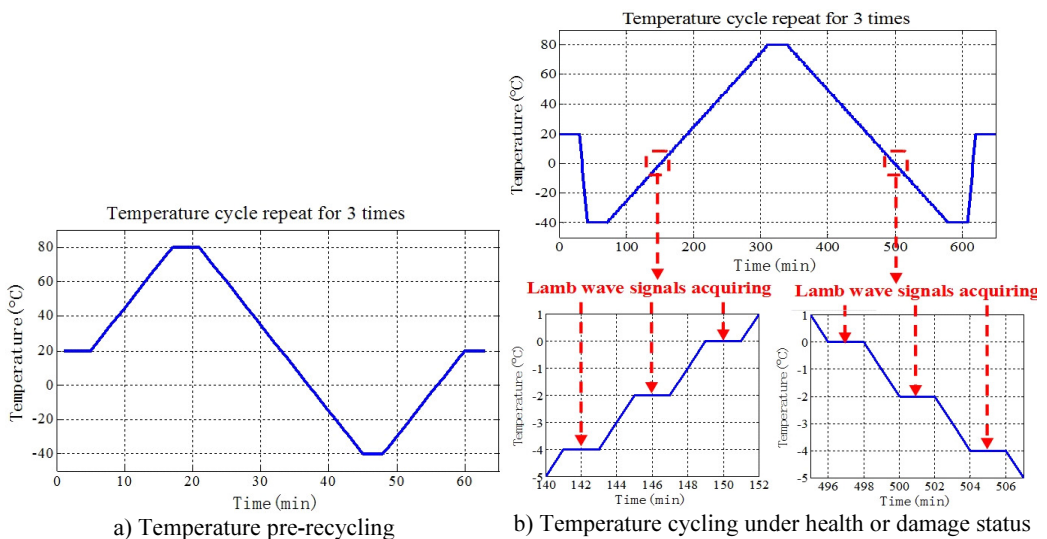


Fig. 2. Temperature cycling illustration

## 2.2. Temperature influence of Lamb wave signals

Fig. 3 gives out a waterfall plot of Lamb wave signals of actuator-sensor channel PZT1-PZT2 of different central frequencies at 20 °C. The first wave packet in the signals is crosstalk signal introduced by the ISS. When the central frequency of excitation signal is low (50 kHz to 100 kHz), the amplitude of  $S_0$  mode is low. But accompanying with the increasing of central frequency, the amplitude of  $S_0$  mode becomes higher. In other words, only  $A_0$  mode should be considered in low frequency. But  $A_0$  and  $S_0$  mode should be both considered in middle and high frequency.

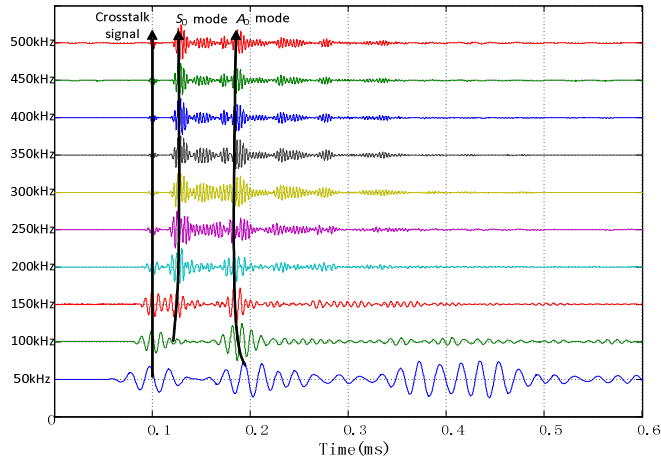
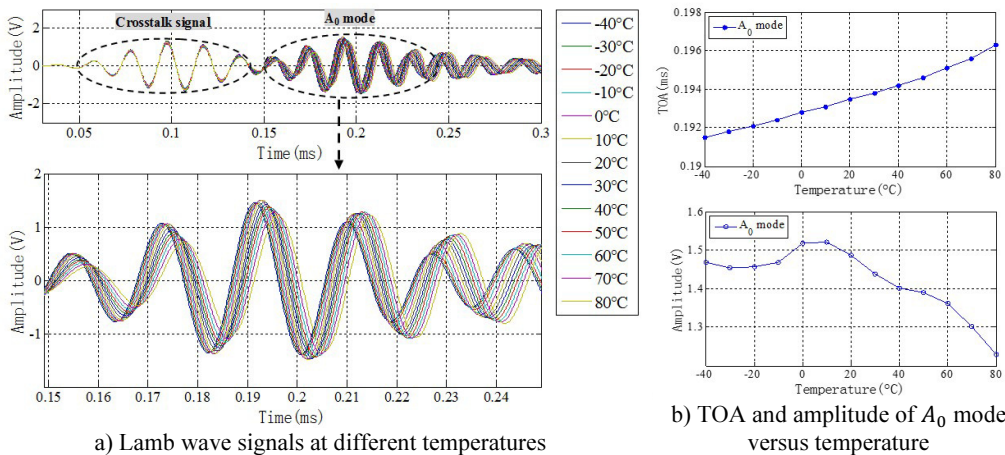


Fig. 3. Mode selection illustration



a) Lamb wave signals at different temperatures

b) TOA and amplitude of  $A_0$  mode versus temperature

Fig. 4. Temperature influence of Lamb wave signals of central frequency 50 kHz

Fig. 4 and 5 show the temperature influence of low and high central frequencies of Lamb wave signals, which come from actuator-sensor channel PZT1-PZT2. The temperature influences on time of arrival (TOA) and amplitude of Lamb wave signals are obvious. TOA has a good linear relationship versus temperature change for both  $S_0$  and  $A_0$  modes of different central frequencies. Temperature change will lead an approximately linear delay to the TOA of Lamb wave signals. Amplitude of  $S_0$  and  $A_0$  modes changed by temperature are more complicated and nonlinear.

Considering the linear relationship versus temperature of TOA and the nonlinear of amplitude, two parameters called as phase changing rate ( $PCR$ , unit  $\text{rad}/^\circ\text{C}$ ) and maximum amplitude variation ( $MAV$ , unit  $\%$ ) are defined to quantify the temperature influence, respectively:

$$PCR = \frac{(TOA_{80^{\circ}\text{C}} - TOA_{-40^{\circ}\text{C}})f_c}{120^{\circ}\text{C}}, \quad (1)$$

$$MAV = \frac{(Amplitude_{\text{max}} - Amplitude_{\text{min}})}{Amplitude_{20^{\circ}\text{C}}} \times 100\%, \quad (2)$$

where  $f_c$  is the central frequency of Lamb wave signals.

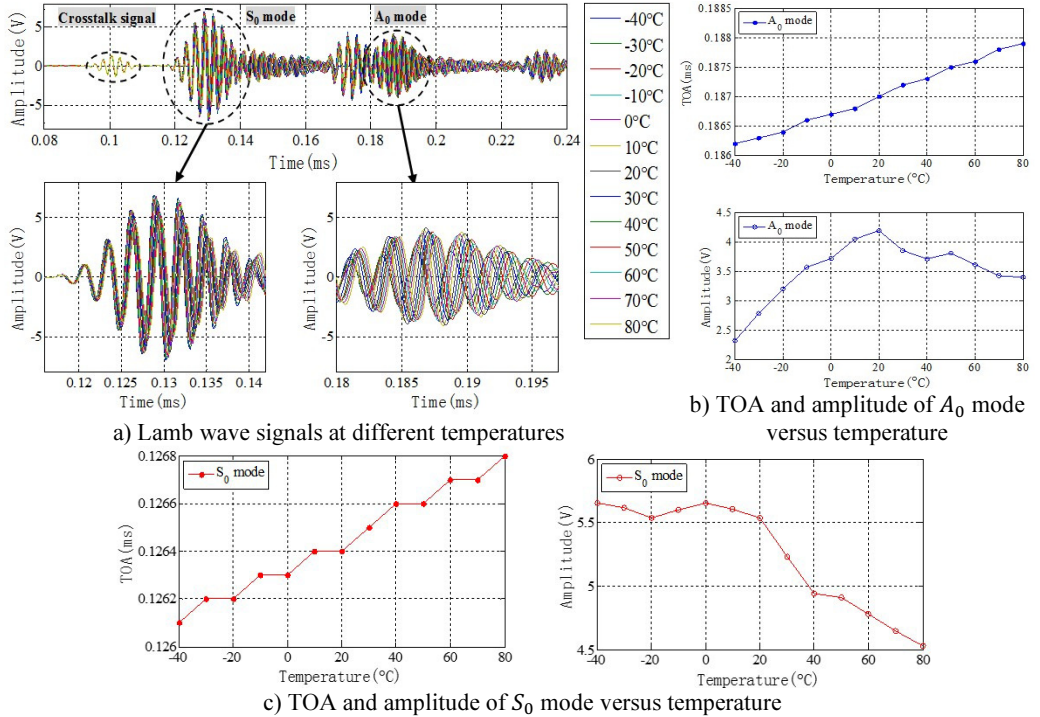


**Fig. 5.** Temperature influence of Lamb wave signals of central frequency 400 kHz

Table 1 lists the two parameters of Lamb wave signals of different central frequencies. It shows that A<sub>0</sub> mode is more sensitive to temperature change than that of S<sub>0</sub> mode. PCR increase accompanying with the increasing of central frequencies. When the central frequency of excitation signal is low (50 kHz to 100 kHz), the amplitude of S<sub>0</sub> mode is very low and the S<sub>0</sub> mode is difficult to observe and analysis.

**Table 1.** PCR and MAV of Lamb wave signals of different central frequencies

Center frequency (kHz)	PCR (rad/°C)		MAV (%)	
	A <sub>0</sub>	S <sub>0</sub>	A <sub>0</sub>	S <sub>0</sub>
50	0.00202	\	19.20	\
100	0.00211	\	40.20	\
150	0.00248	0.00130	83.30	15.32
200	0.00217	0.00133	67.40	31.60
250	0.00350	0.00125	93.90	5.89
300	0.00400	0.00150	43.29	6.09
350	0.00497	0.00175	60.06	14.96
400	0.00567	0.00233	44.78	20.34
450	0.00675	0.00225	39.53	22.10
500	0.00750	0.00250	45.79	54.13

### 3. Temperature compensation method

Most of the SHM methods often use one mode of Lamb wave signal to fulfill damage monitoring task. For example, in damage index based methods [20], direct wave is often used. In damage imaging methods [21], damage scattering signals of  $A_0$  mode or  $S_0$  mode and the corresponding propagation velocity are used. Thus, based on the results of section 2,  $A_0$  mode is selected to be temperature compensated at low central frequency and  $S_0$  mode is selected to be temperature compensated at middle and high central frequency. As the results shown in section 2, temperature change will lead an approximately linear delay to the TOA and nonlinear variation to amplitude. The artificial neural network is often used to solve nonlinear problems. Among the existing artificial neural network, the adaptive filter ADALINE network can attenuate the amplitude and shift the phase of a signal by weighted delay. The function of phase shift of the network can be used to compensate the phase of Lamb wave signals and the function of weight can be used to compensate the amplitude. Thus, this paper adopts the adaptive filter ADALINE network to fulfill the temperature compensation of Lamb wave signals.

#### 3.1. The general idea of the method

The procedure of temperature compensation method is shown in Fig. 6, including adaptive filter ADALINE network construction and temperature compensation with the network.

##### (1) Adaptive filter ADALINE network construction

The whole temperature range from  $-40\text{ }^{\circ}\text{C}$  to  $80\text{ }^{\circ}\text{C}$  is divided into many sub temperature scopes according to compensation standard and accuracy as shown in Fig. 7.

Taking the first temperature scope as an example, a reference temperature  $T_{0R}$  is set to be the central temperature and the Lamb wave signal  $S_{0R}$  at this temperature is set to be the baseline signal. Through the experiment of section 2, the Lamb wave signals at temperature  $T_0, T_{01}, \dots, T_{0i}$  are acquired and set to be  $S_0, S_{01}, \dots, S_{0i}$ .  $S_{0R}$  is considered to be input of adaptive filter ADALINE network and  $S_0, S_{01}, \dots, S_{0i}$  are targets. After training the adaptive filter ADALINE network, a set of network parameters which are weights  $\mathbf{w}_0, \mathbf{w}_{01}, \dots, \mathbf{w}_{0i}$  are acquired.

It should be emphasized that only one baseline signal and a set of weights of adaptive filter ADALINE network are needed to store in each temperature scope.

##### (2) Temperature compensation with the network

In damage monitoring, the environmental temperature and the Lamb wave signal at this temperature are acquired. According to the environmental temperature, the weights of the adaptive filter ADALINE network and the baseline signal are determined. Finally, the baseline signal of the temperature scope is input to the adaptive filter ADALINE network and the output is the compensated baseline signal at the environmental temperature.

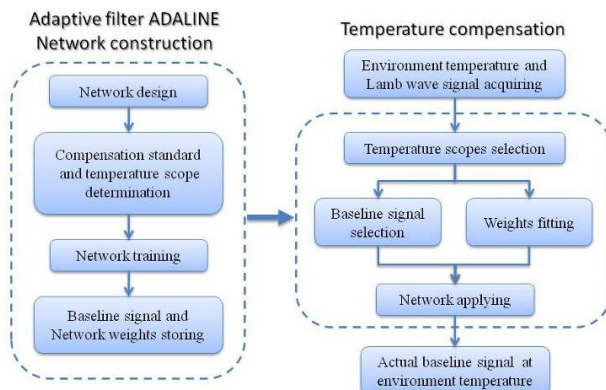


Fig. 6. Procedure of temperature compensation



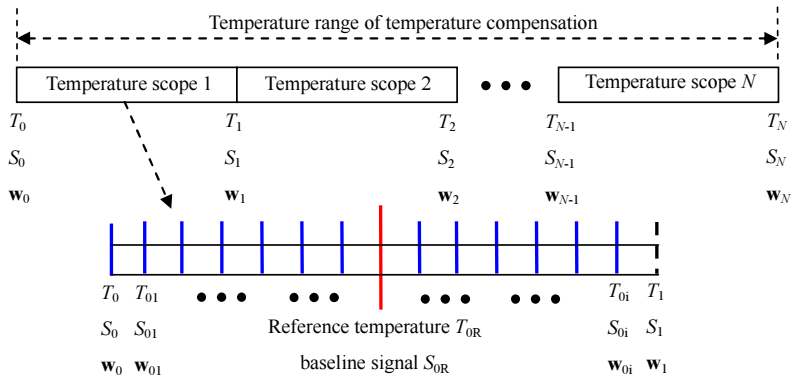


Fig. 7. Temperature scopes illustration

### 3.2. Adaptive filter ADALINE network construction

The architecture of the adaptive filter ADALINE network which contains two layers referred as inputs and ADALINE are shown in Fig. 8. The layer of inputs is consisted of a tapped delay line. The input signal  $f(t)$  enters from the left. At the output of the tapped delay line there is an  $M$ -dimensional vector, consisting of the input signal at the current time and the signals which are tapped delayed from 1 to  $M - 1$  time steps.  $M$  denotes the order of the tapped delay line. The output of the network can be presented as:

$$a(t) = \sum_{m=1}^M w_m f(t - m + 1). \tag{3}$$

In the matrix from:

$$a = \mathbf{w}^T \mathbf{z}, \tag{4}$$

where  $\mathbf{w} = [w_1 \ w_2 \ \dots \ w_M]^T$ ,  $\mathbf{z} = [f(t) \ f(t - 1) \ \dots \ f(t - M + 1)]^T$ .

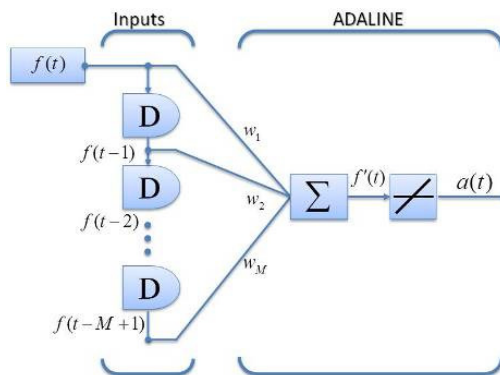


Fig. 8. Network architecture of adaptive filter ADALINE

ADALINE (adaptive liner neural) network is shown in Fig. 8. It has the same basic structure as the perceptron network (one layer). The only difference is that it has a linear transfer.

In this paper, adaptive filter ADALINE network with 2 order tapped delay line ( $M = 2$ ) is selected to fulfill the temperature compensation task. In that case, a neuron with two weights and no bias is sufficient to implement the filter. Such a filter with 2 order tapped delay line can

amplitude-change and phase-shift Lamb wave signal in the desired way. According to our research,  $M$  is recommended set to be 2 for Lamb wave signal. Because ADALINE network with 2 orders tapped delay line is simple and easy to train. On the other side, when  $M$  is set to be 3 or more than 3, the training results are not getting better and the weights become nonlinear to temperature.

The structure of adaptive filter ADALINE network is a classical uniform embedding with constant time lag equal to 1 which is capable to conduct amplitude-change and phase-shift Lamb wave signal in the desired way. Further study can be conducted on non-uniform embedding. The optimal time lags and optimal embedding dimensions for non-uniform embedding can be determined with the method proposed in [22].

In SHM applications, damage can be determined by evaluating maximum error of subtracted signal between monitoring signal and baseline signal. In that case, a normalized maximum error  $Er$  is used to be the compensation standard and to validate the compensation results as shown in Eq. (5). It is a minimization criterion of the maximum amplitude to compare the similarity of the time domain signal:

$$Er = 20 \lg \left( \frac{\max(|a(t) - f_T(t)|)}{\max(|f_T(t)|)} \right), \quad (5)$$

where  $a(t)$  is the output of the network,  $f_T(t)$  is the target Lamb wave signal.

According to the Lamb wave signals acquired in health and damage status in section 2, the maximum error of their subtracted signals are  $-5.25$  dB (PZT5-PZT9) and  $-29.78$  dB (PZT1-PZT2). Combining the results from the research of Roy [14], temperature compensation standard is set as  $Er < -25$  dB. In this case, the temperature scope for  $A_0$  mode is set as  $20$  °C and it is  $12$  °C for  $S_0$  mode.

Based on the compensation standard and the Lamb wave signals acquired in section 2, the network training for one temperature in one temperature scope can be performed. The goal of network training is to minimize the mean square error (MSE) of the target  $f_T(t)$  and the output  $a(t)$ . The training function is the least mean square (LMS) algorithm [23].

The MSE of the network can be expressed as Eq. (6):

$$F(\mathbf{w}) = E(e^2) = E \left[ (f_T(t) - a(t))^2 \right] = E[(t - \mathbf{w}^T \mathbf{z})^2]. \quad (6)$$

Here  $E[\ ]$  is expectation. This expression can be expanded and simplified to Eq. (7):

$$F(\mathbf{w}) = c - 2\mathbf{w}^T \mathbf{h} + \mathbf{w}^T \mathbf{R} \mathbf{w}, \quad (7)$$

where  $c = E[t^2]$ ,  $\mathbf{h} = E[t\mathbf{z}]$ ,  $\mathbf{R} = E[\mathbf{z}\mathbf{z}^T]$ .

The gradient of MSE can be expressed as Eq. (8):

$$\nabla F(\mathbf{w}) = \nabla(c - 2\mathbf{w}^T \mathbf{h} + \mathbf{w}^T \mathbf{R} \mathbf{w}) = -2\mathbf{h} + 2\mathbf{R}\mathbf{w}. \quad (8)$$

The LMS algorithm, with a constant learning rate  $\alpha$ , can be written as Eq. (9):

$$\mathbf{w}_{k+1} = \mathbf{w}_k - \alpha \nabla F(\mathbf{w})|_{\mathbf{w}=\mathbf{w}_k}. \quad (9)$$

The learning rate can be set according to the following Eq. (10), (11) and (12):

$$\mathbf{w}_{k+1} = \mathbf{w}_k - \alpha[-2\mathbf{h} + 2\mathbf{R}\mathbf{w}] = [\mathbf{I} - 2\alpha\mathbf{R}]\mathbf{w}_k + 2\alpha\mathbf{h}, \quad (10)$$

$$1 - 2\alpha\lambda_i > -1, \quad (11)$$

where  $\lambda_i$  are the eigenvalues of  $\mathbf{R}$ .



$$0 < \alpha < 1/\lambda_{\max} \tag{12}$$

In this paper, the learning rate is set as be 0.0005.

For example, in order to obtain the weights at 20 °C, the 4th temperature scope is selected and the reference temperature is set as 30 °C. Thus, Lamb wave signal at 30 °C is set to be the input of the network, while the signal at 20 °C is the target of the network.

In section 2, six groups of Lamb wave health signals are acquired. Three samples of them are used for training the network, while the other three samples are used for testing the network with the compensation standard. The three samples of Lamb wave signals for training the network are set as input of the neural repeatedly until the weight matrix  $\mathbf{w}$  converges. The weights of the network are an optimal solution for all the three samples after training.

The training convergence curve is shown in Fig. 9. After 30 thousand iteration steps, the weights is converges to  $(-3.57, 4.567)$  and the  $MES$  converges to  $1.6 \times 10^{-3}$ . After training, the normalized maximum errors between output and target is  $-28$  dB which is less than  $-25$  dB and meet the compensation standard. Through the process mentioned above, the weights of adaptive filter ADALINE network for one temperature in one temperature scope are obtained.

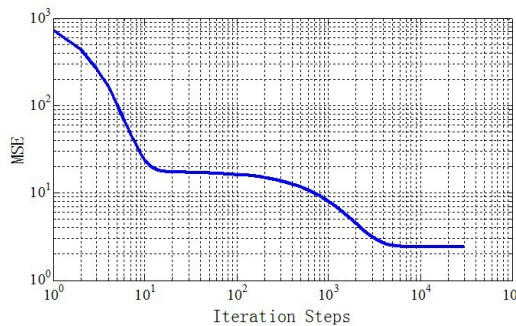


Fig. 9. Convergence curve of network training of one temperature in one temperature scope

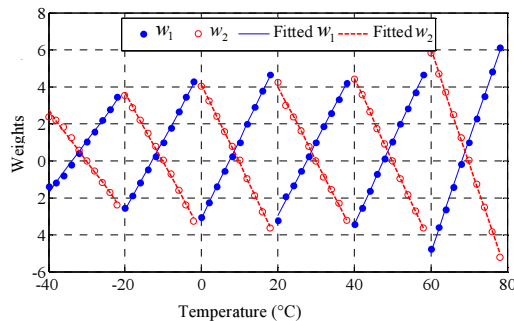


Fig. 10. Weights changed with temperature

The weights of the network at the other temperature in each temperature scope can be obtained in the same way. The network architecture for each temperature is the same, while the weights of the network are altered according to the monitoring temperature.

As the temperature acquired by a temperature sensor is not always integers, there is great importance to fit the weights to improve accuracy. As shown the solid blue line in Fig. 10, the weights are linear to temperature at each temperature scope. Thus, the least square linear fit is implemented to fit the weights which are shown the dotted red line in Fig. 10.

Once a set of weights are obtained and their performance meet the compensation standard, they can be adopted in adaptive filter ADALINE network to temperature compensation which is based on Eq. (4).

## 4. Temperature compensation method validation

### 4.1. Temperature compensation of $A_0$ mode

According to the compensation standards and requirements, temperature compensation scope for  $A_0$  mode is determined as 20 °C. Lamb wave signals of six reference temperatures (which are -30 °C, -10 °C, 10 °C, 30 °C, 50 °C, 70 °C) are acquired and stored in the baseline signal database. The weights are trained and fitted to obtain the weights at each temperature.

Then according to the environmental temperature, the weights of the adaptive filter ADALINE network and the baseline signal are determined. Finally, the baseline signal of the temperature scope is input to the adaptive filter ADALINE network and the output is the compensated baseline signal at the environmental temperature.

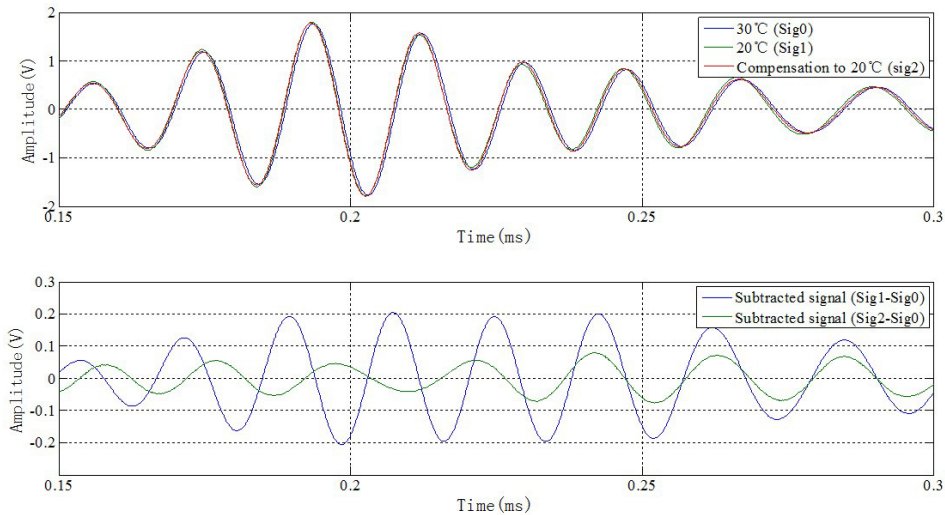


**Fig. 11.** Compensate baseline signal (30 °C) to target signal (20 °C)

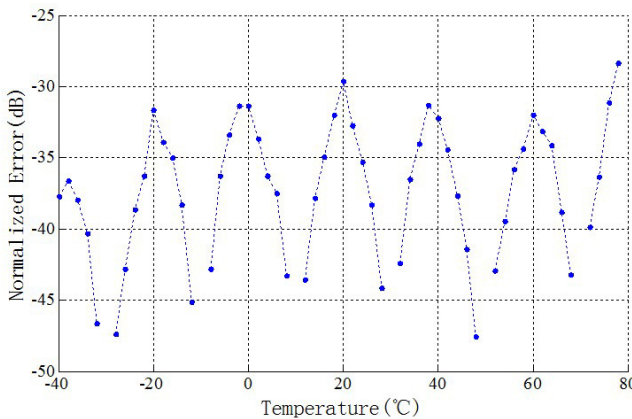


**Fig. 12.**  $A_0$  mode compensation result

For example, the environment temperature is at 20 °C. In that case, the fourth temperature scope is selected and the reference temperature for this scope is 30 °C. Thus, baseline signal at 30 °C is selected as the input of the network. On the other hand, the network weights for 20 °C are selected from the set of weights trained in section 3. After applying the network, the output of the network is the compensated signal at 20 °C, as shown in Fig. 11. The figure illustrates that the

amplitude of subtracted signal between Lamb wave signals obtained 20 °C and 30 °C is up to 0.2 V, while after compensation it is less than 0.07 V (normalized maximum error is -28 dB) which meet the compensation standard.

For compensating the signal at other temperature, the same algorithm can be used. The compensation results are verified at each temperature as illustrated in Fig. 12. In stiffened composite panel, temperature varies from -40 °C to 80 °C, temperature compensation scope of baseline signal is set as 20 °C for  $A_0$  mode. After compensation, the normalized maximum errors are less than -25 dB at each temperature.

#### 4.2. Temperature compensation of $S_0$ mode

According to the compensation standards and requirements, temperature compensation scope for  $S_0$  mode is determined as 12 °C. Lamb wave signals of ten reference temperatures (which are -34 °C, -22 °C, -10 °C, 2 °C, 14 °C, 26 °C, 38 °C, 50 °C, 62 °C, 74 °C) are acquired and stored in the baseline signal database. The weights are trained and fitted to obtain the weights at each temperature.

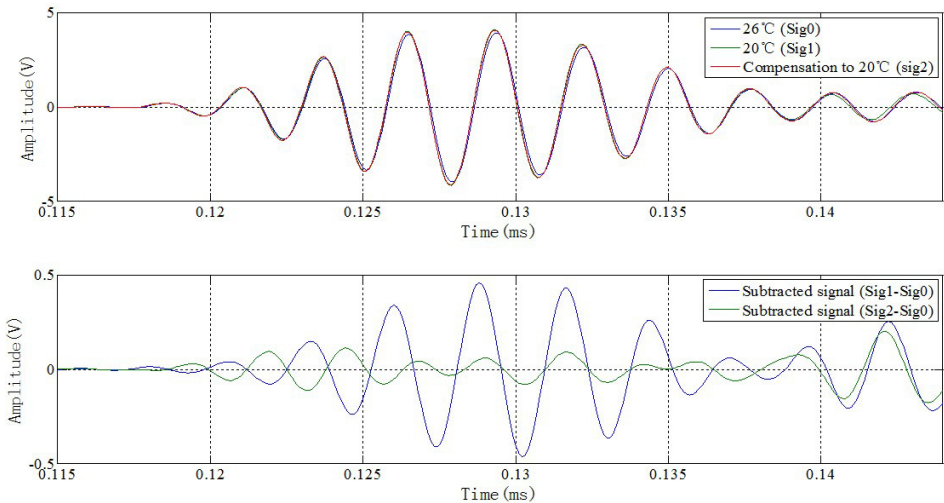


Fig. 13. Compensate baseline signal (26 °C) to target signal (20 °C)

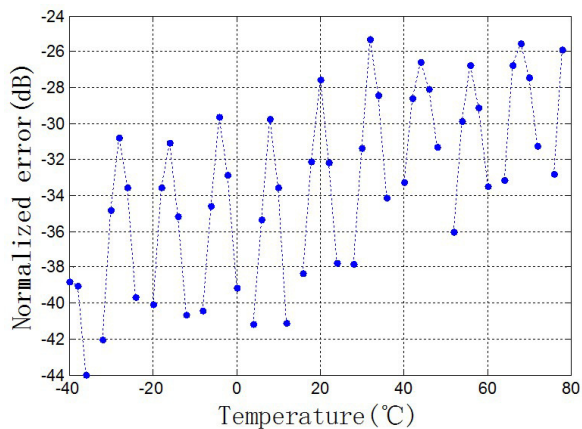


Fig. 14.  $S_0$  mode compensation result

The method compensate for  $S_0$  mode is the same as  $A_0$  mode. For example, the environment

temperature is at 20 °C. In that case, the sixth temperature scope is selected and the reference temperature for this scope is 26 °C. Thus, the baseline signal at 26 °C is selected as the input of the network. On the other hand, the network weights for 20 °C are selected from the set of weights trained in section 3. After applying the network, the output of the network is the compensated signal at 20 °C, as shown in Fig. 13.

For compensating the signal at other temperature, the same algorithm can be used. The compensation results are verified at each temperature as illustrated in Fig. 14. In stiffened composite panel, temperature various from -40 °C to 80 °C, temperature compensation scope of baseline signal is set as 12 °C for  $S_0$  mode. After compensation, the normalized maximum errors are less than -25 dB at each temperature.

### 4.3. Damage imaging combination with temperature compensation

The delay-and-sum imaging algorithm [21, 24] is applied in this section to determined the health status of the monitoring area. The algorithm compares the signal of the structure at health and damage status and determines the damage location. The actual damage is located in the center of the area surrounded by PZT 5, PZT 6, PZT 8 and PZT 9 and coordinate of the damage is (-75 mm, -42.5 mm).

With the signals recorded in section 2, four typical conditions for engineering application are demonstrated in the following to validate compensation results.

#### (1) Temperature effect cause false alarms

When the temperature changes, even the structure are not damaged, the algorithm shows false alarms. For example, the health signal at 20 °C is set to be Health Signal of the imaging algorithm, while the health signal at 30 °C is set to be Damage Signal. The imaging result shows a false damage in (160 mm, 104 mm) as demonstrated in Fig. 15a. The point with the pixel peak value of the imaging result is often regarded as the damage location.

#### (2) Image result without compensation

Another condition is that under the influence of temperature, even the structure is damaged, the algorithm cannot determine the right location of damage. An example is given: the health signal at 20 °C is set to be Health Signal of the imaging algorithm, while the damage signal at 30 °C is set to be Damage Signal. The imaging result shows damage located in (172 mm, -15 mm) as demonstrated in Fig. 15b. The damage information is concealed by temperature effect. The result shows that it is very important to conduct temperature compensation.

#### (3) Image result with compensation

In this condition, the health signal at baseline temperature is compensated to health signal at the target temperature. For example, the ADALINE network is applied to compensate the health signal at 20 °C to the compensational health signal at 30 °C. The compensational health signal at 30 °C is set to be Health Signal of the imaging algorithm, while the damage signal at 30 °C is set to be Damage Signal. The imaging result shows a damage in (-70 mm, -44 mm) as demonstrated in Fig. 15c. The result shows that after compensation, great accuracy is acquired with an error of 5.2 mm.

#### (4) Traditional damage detection

In the last condition, the health signal is recorded at the target temperature and is used in damage imaging with the damage signal at target temperature. The health signal at 30 °C is set to be Health Signal of the imaging algorithm, while the damage signal at 30 °C is set to be Damage Signal. The imaging result shows a damage in (-70 mm, -43 mm) as demonstrated in Fig. 15d. The result shows that the damage image result is the same as the compensated result.

Generally speaking, temperature effects will cause false alarms and conceal the damage information. After compensation, great accuracy is acquired with an error of 5.2 mm. The proposed temperature compensation method is effective and has been verified by the damage detection.

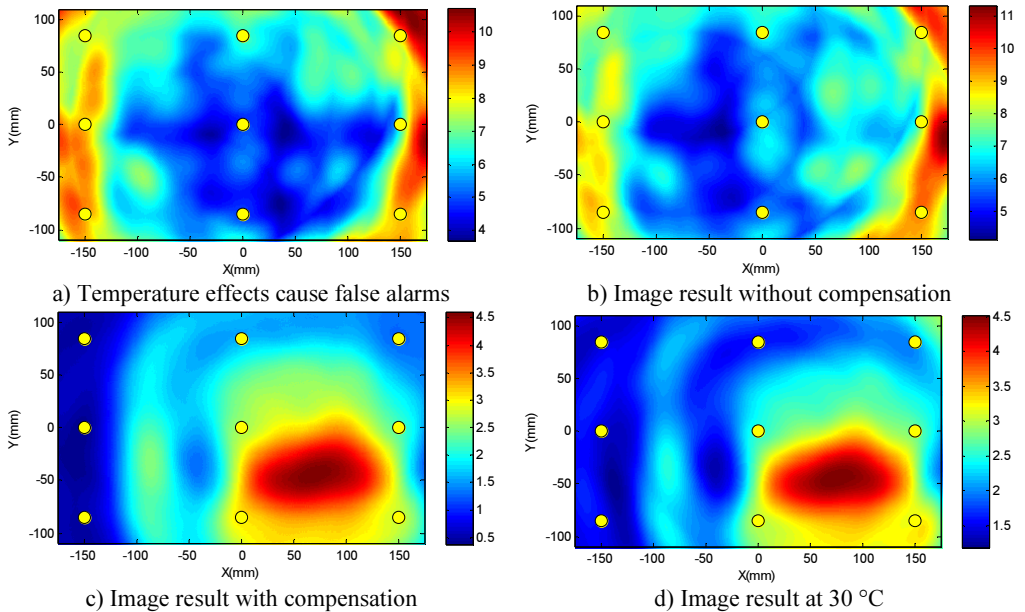


Fig. 15. Damage imaging results

## 5. Conclusions

In this paper, a new temperature compensation method based on adaptive filter ADALINE network has been developed to compensate the amplitude-change and phase-shift of Lamb wave signals caused by temperature. The advantage of this temperature compensation method is that only a few baseline signals are required for a large temperature range.

Experiments are conducted on a stiffened carbon fiber composite panel to verify the temperature compensation method in a large temperature range from  $-40\text{ }^{\circ}\text{C}$  to  $80\text{ }^{\circ}\text{C}$ . Results show that in order to provide good temperature compensation with the proposed method, the temperature compensation scope can be set to  $20\text{ }^{\circ}\text{C}$  for  $A_0$  mode Lamb wave signal, while it can be set to  $12\text{ }^{\circ}\text{C}$  for  $S_0$  mode Lamb wave signal. Damage image results shows that after the compensation great accuracy for Lamb wave-based damage detection is achieved.

This temperature compensate technique can be applied for both composite structures and metallic structures. When this technique is applied to a new structure, the weights for ADALINE network at each temperature should be retrained with the data acquired in this new structure. In other words, the same procedure should be conducted as shown in Fig. 6. The next steps of this research are to extend the present work for real composite structures with high geometric complexity.

## Acknowledgements

This work is supported by the National Science Fund for Distinguished Young Scholars (Grant No. 51225502), the National Natural Science Foundation of China (Grant No. 51205189) and China Postdoctoral Science Foundation (Grant No. 2012M510183).

## References

- [1] **Diamanti K., Soutis C.** Structural health monitoring techniques for aircraft composite structures. *Progress in Aerospace Sciences*, Vol. 46, Issue 8, 2010, p. 342-352.

- [2] **Staszewski W., Mahzan S., Traynor R.** Health monitoring of aerospace composite structures – active and passive approach. *Composites Science and Technology*, Vol. 69, Issue 11-12, 2009, p. 1678-1685.
- [3] **Staszewski W., Boller C., Tomlinson G. R.** Health Monitoring of Aerospace Structures: Smart Sensor Technologies and Signal Processing. Wiley, 2004.
- [4] **Giurgiutiu V., Santoni-Bottai G.** Structural health monitoring of composite structures with piezoelectric-wafer active sensors. *AIAA Journal*, Vol. 49, Issue 11, 2011, p. 565-581.
- [5] **Lee B., Manson G., Staszewski W.** Environmental effects on Lamb wave responses from piezoceramic sensors. *Materials Science Forum*, Trans. Tech. Publ., Vol. 440, 2003, p. 152-202.
- [6] **Qing X. P., Beard S. J., Kumar A., Sullivan K., Aguilar R., Merchant M., et al.** The performance of a piezoelectric-sensor-based SHM system under a combined cryogenic temperature and vibration environment. *Smart Materials and Structures*, Vol. 17, Issue 5, 2008, p. 055010.
- [7] **Mustapha F., Mohd A. K. D., Wardi N. A., Sultan M. T. H., Shahrjerdi A.** Structural health monitoring (SHM) for composite structure undergoing tensile and thermal testing. *Journal of Vibroengineering*, Vol. 14, Issue 3, 2012, p. 1342-1353.
- [8] **Sohn H.** Effects of environmental and operational variability on structural health monitoring. *Philosophical Transactions of the Royal Society A: Mathematical, Physical and Engineering Sciences*, Vol. 365, Issue 1851, 2007, p. 539-560.
- [9] **Raghavan A., Cesnik C. E.** Studies on effects of elevated temperature for guided-wave structural health monitoring. *The 14th International Symposium on Smart Structures and Materials & Nondestructive Evaluation and Health Monitoring*, International Society for Optics and Photonics, Vol. 6529, 2007, p. 65290A-1-12.
- [10] **Clarke T., Simonetti F., Cawley P.** Guided wave health monitoring of complex structures by sparse array systems: influence of temperature changes on performance. *Journal of Sound and Vibration*, Vol. 329, Issue 12, 2010, p. 2306-2322.
- [11] **Croxford A. J., Moll J., Wilcox P. D., Michaels J. E.** Efficient temperature compensation strategies for guided wave structural health monitoring. *Ultrasonics*, Vol. 50, Issue 4-5, 2010, p. 517-528.
- [12] **Konstantinidis G., Wilcox P. D., Drinkwater B. W.** An investigation into the temperature stability of a guided wave structural health monitoring system using permanently attached sensors. *Sensors Journal*, IEEE, Vol. 7, Issue 5, 2007, p. 905-912.
- [13] **Lu Y., Michaels J. E.** A methodology for structural health monitoring with diffuse ultrasonic waves in the presence of temperature variations. *Ultrasonics*, Vol. 43, Issue 9, 2005, p. 713-731.
- [14] **Roy S., Lonkar K., Janpati V., Chang F. K.** Physics based temperature compensation strategy for structural health monitoring. *8th International Workshop on Structural Health Monitoring*, Stanford University, CA, 2011.
- [15] **Salamone S., Bartoli I., Lanza Di S. F., Coccia S.** Guided-wave health monitoring of aircraft composite panels under changing temperature. *Journal of Intelligent Material Systems and Structures*, Vol. 20, Issue 9, 2009, p. 1079-1090.
- [16] **Marzani A., Salamone S.** Numerical prediction and experimental verification of temperature effect on plate waves generated and received by piezoceramic sensors. *Mechanical Systems and Signal Processing*, Vol. 30, 2012, p. 204-217.
- [17] **Dodson J. C., Inman D. J.** Thermal sensitivity of Lamb waves for structural health monitoring applications. *Ultrasonics*, Vol. 53, Issue 3, 2013, p. 677-658.
- [18] **Zhang X., Yuan S., Liu M., Yang W.** Analytical modeling of Lamb wave propagation in composite laminate bonded with piezoelectric actuator based on Mindlin plate theory. *Journal of Vibroengineering*, Vol. 14, Issue 4, 2012, p. 1681-1700.
- [19] **Qiu L., Yuan S.** On development of a multi-channel PZT array scanning system and its evaluating application on UAV wing box. *Sensors and Actuators A: Physical*, Vol. 151, Issue 2, 2009, p. 220-230.
- [20] **Feng Y., Yang J., Chen W.** Delamination detection in composite beams using a transient wave analysis method. *Journal of Vibroengineering*, Vol. 15, Issue 1, 2013, p. 139-151.
- [21] **Michaels J. E.** Detection, localization and characterization of damage in plates with an in situ array of spatially distributed ultrasonic sensors. *Smart Materials and Structures*, Vol. 17, Issue 3, 2008, p. 035035.
- [22] **Ragulskis M., Lukoseviciute K.** Non-uniform attractor embedding for time series forecasting by fuzzy inference systems. *Neurocomputing*, Vol. 72, Issue 10-12, 2009, p. 2618-2626.
- [23] **Hagan M. T., Demuth H. B., Beale M. H.** *Neural Network Design*. Thomson Learning Stamford, CT, 1996.
- [24] **Qiu L., Liu M., Qing X., Yuan S.** A quantitative multi-damage monitoring method for large-scale complex composite. *Structural Health Monitoring*, Vol. 12, Issue 3, 2013, p. 183-196.